Available online at www.sciencedirect.com
ScienceDirect
Journal of Sound and Vibration 314 (2008) 343–356
JOURNAL OF SOUND AND VIBRATION
www.elsevier.com/locate/jsvi

Identification of modal parameters from transmissibility measurements

Christof Devriendt*, Patrick Guillaume

Vrije Universiteit Brussel, Department of Mechanical Engineering, Acoustics and Vibration Research Group, 1050 Brussels, Belgium

Received 21 July 2006; received in revised form 31 October 2007; accepted 17 December 2007
Available online 11 February 2008

Abstract

It is a well-known fact that linear dynamic behavior of structures can be studied by modeling the relation between force(s) [input(s)], acting on a structure, and their resulting structural vibration response(s) [output(s)]. For industrial structures, in their real in-operation conditions, it often becomes hard (or impossible) to experimentally measure the excitation. For this reason system identification techniques have been developed that work on a basis of response data only. However, current output only techniques have serious limitations when applied to some practical cases. One limiting constraint of the current OMA techniques is that the non-measured excitations to the system in operation must be white-noise sequences. In practice however, structural vibrations observed in operation cannot always be considered as pure white-noise excitation. Current techniques may encounter difficulties to correctly identify the modal parameters. In this paper a new OMA approach to identify modal parameters from output-only transmissibility measurements is introduced. This method does not make any assumption about the nature of the excitations to the system. In general, the poles that are identified from transmissibility measurements do not correspond with the system's poles. However, by combining transmissibility measurements under different loading conditions, it is shown in this paper that modal parameters can be identified. In this contribution a numerical experiment on a cantilever beam was conducted. A comparison was made between the results of a classic input–output and the new output-only modal analysis based on transmissibility measurements.

1. Introduction

During the last two decades, research has developed a growing interest for the domain of modal analysis. Experimental modal testing has become a commonly used technique for studying the behavior of mechanical and civil structures such as cars, aircraft and bridges, offshore platforms and industrial machinery. During a classic modal test, both the artificially applied forces and resulting structural vibration responses are measured. On the basis of this data, a modal model of the structure, that essentially contains the same information as the original vibration data, is derived by means of system identification [1–3]. The appropriateness of the parametric model for physical interpretation makes scientists and engineers most often prefer this type of model for their structural dynamics research. Obtaining a modal model of the structure is

*Corresponding author.
E-mail address: cdevrien@vub.ac.be (C. Devriendt).
URL: http://www.avrg.vub.ac.be (C. Devriendt).

0022-460X/$ - see front matter © 2007 Elsevier Ltd. All rights reserved.
doi:10.1016/j.jsv.2007.12.022

often not the final goal, but only a means to get valuable information for use with other applications. Examples of such applications are given by: design/redesign of prototypes; finite element model updating; damage detection and structural health monitoring. A detailed overview of classic modal analysis theory can be found in Refs. [4–6]. Starting from 1996, the identification of output-only vibration data from mechanical structures received a considerable amount of attention. Adapting model-based system identification techniques [e.g. maximum likelihood (ML) estimator, least-squares complex exponential (LSCE) estimator, sub-space-based techniques] for use with output only data, has created the possibility to identify the modal models from in-operation mechanical structures excited by ambient noise and vibration [1,8–10]. The modeling of the dynamic behavior of structures from output-only vibration data, has become a valid alternative for structures where a classic forced-vibration test would be difficult, if not impossible, to conduct. The use of in-operations modal analysis is particularly interesting because the structure remains in its normal in-operating condition during the test. This can be considered an important advantage, since the conditions during a laboratory forced-vibration test are often significantly different from the real in operation working conditions. However, current output only techniques have serious limitations when applied to some practical cases. One limiting constraint of the current OMA techniques is that the non-measured excitations to the system in operation must be white-noise sequences. In practice however, structural vibrations observed in operation cannot always be considered as pure white-noise excitation. In many mechanical structures the loading forces are often more complex and even harmonic components can be present in the response. This is especially true, when measuring on mechanical structures containing rotating parts (e.g. cars, turbines, windmills), but also civil engineering structures may have responses superimposed by harmonic components. OMA procedures are, strictly speaking, not applicable in these situations. Current techniques may encounter difficulties to correctly identify the modal parameters [11]. The non-random force contributions are sometimes wrongly identified as physical modes. The art is then to distinguish real structural behavior from noise and excitation contributions. In order to separate the true structural modes from the forced excitation components, a number of techniques can be used. For separating, e.g., harmonic components, special numerical filters can be applied to filter-out those components or indicators to identify them can be used [12]. Unfortunately, in practice many of those procedures fail if the harmonic frequencies are close to the eigenfrequencies of the structure or when the strength of the signal arising from harmonic excitations is very high compared to the response associated with the eigenfrequencies of the structure excited through the noise input. In most practical cases filtering pollutes the measured response and significantly changes the poles of the structural modes so that the identified modal parameters are perturbed. In Ref. [13] the authors define an indicator to easily identify harmonics from the signal when the frequency domain decomposition is applied. In a next step, before estimating the single-degree of-freedom (sdof) function, they remove the peaks caused by these harmonics by using a linear interpolation. This approach estimates, in general, the natural frequencies and damping ratios with a good accuracy. However, when the harmonic component is close to the natural frequency, larger deviations occur. Especially in lightly damped structures the obtained damping ratio is higher as the calculated sdof function gets more 'flat' due to this linear interpolation. The authors propose a polynomial fit to improve the current results. Other techniques start from the assumption that those harmonic force contributions can always be considered as non-damped modes in addition to the natural modes of the structure. In Refs. [14,15], modified modal analysis methods where the harmonic excitation components are explicitly taken into account during the identification are proposed. These methods allow modal parameters to be computed accurately even if the harmonic frequencies are close to the eigenfrequencies, but assume that the harmonic frequencies are known a priori.

In this paper a new OMA technique based on transmissibility measurements will be applied. This method does not make any assumption about the nature of forces and reduces the risk of wrongly identifying the modal parameters due to the presence of non-white-noise sequences. In this contribution, both input–output and output-only numerical vibration experiments were conducted on a cantilever beam in order to study the applicability of the output-only identification technique using transmissibility measurements. In the next section different parametric models in the frequency domain to describe the dynamical behavior of vibrating structures are introduced. Next, the deterministic approach for the experimental modal analysis case and a stochastic approach for the operational modal analysis case are discussed, to introduce the new stochastic approach based on transmissibility measurements in Section 3.

2. Parametric models

2.1. The modal model

Newton's equations of motion for a finite-dimensional linear structure are a set of N_m second-order differential equations, where N_m is the number of independent degrees-of-freedom (dofs), given by

$$\mathbf{M}\ddot{x}(t) + \mathbf{C}_1\dot{x}(t) + \mathbf{K}x(t) = f(t), \tag{1}$$

with $\mathbf{M}$, $\mathbf{C}$ and $\mathbf{K} \in \mathbb{R}^{N_m \times N_m}$, respectively the mass, damping and stiffness matrices, $f(t) \in \mathbb{R}^{N_m \times 1}$ the applied force and $x(t) \in \mathbb{R}^{N_m \times 1}$ the structure's displacement response. Using the Laplace transform and neglecting the initial conditions results in the frequency-domain equivalent given by

$$\mathbf{Z}(s)\mathbf{X}(s) = \mathbf{F}(s), \tag{2}$$

with the dynamical stiffness $\mathbf{Z}(s) = \mathbf{M}s^2 + \mathbf{C}_1 s + \mathbf{K}$. Inverting Eq. (2) yields

$$\mathbf{X}(s) = \mathbf{H}(s)\mathbf{F}(s), \tag{3}$$

with $\mathbf{H}(s) = (\mathbf{Z}(s))^{-1}$ the transfer function matrix. The transfer function matrix can be formulated in its modal form [4,5]

$$\mathbf{H}(s) = \boldsymbol{\phi}[s\mathbf{I}_{N_m} - \boldsymbol{\Lambda}]^{-1}\mathbf{L}^{\mathrm{T}} + \boldsymbol{\phi}^{*}[s\mathbf{I}_{N_m} - \boldsymbol{\Lambda}^{*}]^{-1}\mathbf{L}^{*}, \tag{4}$$

with the diagonal matrix $\boldsymbol{\Lambda}$ given by

$$\boldsymbol{\Lambda} = \mathrm{diag}(\{\lambda_1, \lambda_2, \ldots, \lambda_{N_m}\}) \tag{5}$$

and N_m the number of modes. The modal parameters λ_r, $\phi_{[:,r]}$ and $L_{[:,r]}$ are, respectively, the pole, mode shape and modal participation factor of mode r. The mathematical operators transpose, complex conjugate and hermitian conjugate are, respectively, denoted as $[.]^{\mathrm{T}}$, $[.]^{*}$ and $[.]^{H}$. The poles $\lambda_r = \sigma_r + \mathrm{j}\omega_r$ contain the natural frequencies $f_r = \omega_r/(2\pi)$ and the damping ratios $d_r = -\sigma_r/(\sigma_r^2 + \omega_r^2)$. The complex operator is denoted as j.

From an engineering point of view the modal model of a structure provides the best physical understanding. It describes the vibration behavior of a structure with a limited number of parameters. However, since this model is highly nonlinear in its parameters most identification algorithms do not directly identify the modal parameters. Most modal parameters estimation methods identify first a rational polynomial matrix-fraction modal. This modal model can be related to the physical parameters of the modal model in a second step. The common-denominator model, or scalar matrix-fraction description, is such a model and is discussed in the next section.

2.2. Common-denominator model

The common denominator, also called scalar matrix-fraction model, considers the relation between output o and input i as a rational fraction of two polynomials, of which the denominator polynomial is common for all input–output relations [7]. The transfer function matrix $H(s)$ can be expressed as

$$\mathbf{H}(s) = \frac{\mathbf{Z}_{\mathrm{adj}}(s)}{|Z(s)|}, \tag{6}$$

with $\mathbf{Z}_{\mathrm{adj}}(s)$ the adjoint matrix, containing polynomials of order $2(N_m - 1)$. The common-denominator is then given by the characteristic equation $|Z(s)|$, a polynomial in s of order $2N_m$, whose roots are the poles of the structure. In general the common-denominator model can be expressed as

$$\mathbf{H}(s) = \frac{\begin{bmatrix} B_{11}(s) & \ldots & B_{1N_i}(s) \\ \vdots & \ddots & \vdots \\ B_{N_o1}(s) & \ldots & B_{N_oN_i}(s) \end{bmatrix}}{A(s)}, \tag{7}$$

The relation between the modal model and the common-denominator model is obtained by considering the frequency response function (FRF) between output o and input i

$$H_{oi}(s) = \frac{B_{oi}(s)}{A(s)} = \sum_{r=1}^{N_m} \left(\frac{\phi_{or} L_{ir}}{s - \lambda_r} + \frac{\phi_{or}^* L_{ir}^*}{s - \lambda_r^*} \right) \tag{8}$$

From this equality it is clear that the structure poles are given by the roots of the denominator $A(s)$, while the mode shapes and participation factors are obtained from a singular value decomposition of the residue matrix $\mathbf{A}_r \in \mathbb{C}^{N_o \times N_i}$ of mode r.

$$\mathbf{A}_r = \boldsymbol{\phi}_r \mathbf{L}_r^{\mathrm{T}}, \tag{9}$$

with the elements of the residue matrix $\mathbf{A}_r$ given by

$$a_{oi,r} = \lim_{s \to \lambda_r} (s - \lambda_r) \frac{B_{oi}(s)}{A(s)} = \phi_{or} L_{ir} \tag{10}$$

and $\phi_r = [\phi_{1r} \phi_{2r} \ldots \phi_{N_o r}]^{\mathrm{T}}$, $L_r = [L_{1r} L_{2r} \ldots L_{N_o r}]^{\mathrm{T}}$.

3. Primary identification data

In the previous paragraph the modal model and the common-denominator model and their relation was introduced. In this section attention will be paid to the primary data from which one usually starts to identify a mathematical model. A distinction is made between the availability of input–output measurements or only output measurements. Finally, the new approach of operational modal analysis using transmissibility measurements as primary data is introduced as a generalization of the applicability of current output-only methods.

3.1. Input–Output measurements: a deterministic approach

Linear time-invariant systems can be modeled by starting from input–output measurements. The identified parametric model essentially contains the same information of the studied system as the original non-parametric data, but is often preferred because of its compact form and possible physical interpretation. Several important references on the subject of system identification include Refs. [2,1] for time-domain identification and [3] for frequency-domain identification.

The application of system identification techniques to the identification of modal models–natural frequencies, damping ratios, mode shapes and modal participation factors–starting from input–output measurements is known as *experimental modal analysis* (EMA). Many textbooks give an extensive overview of EMA and input-output modal parameter estimation method [4–6]. As mentioned in the introduction, these experimentally determined modal models can be used in a wide range of structural dynamics applications.

EMA starts from identifying modal models from the measured applied forces and vibration responses of the structure, when artificially excited in one or more locations (illustrated by Fig. 1). These experiments are performed under laboratory conditions to obtain high-quality measurements. From these input–output measurements a mathematical model is identified, which is converted to a modal model of the structure.

3.1.1. FRF-based experimental modal analysis

In the field of system identification, most identification algorithms start from the measured input and output time histories, or in the case of frequency-domain identification algorithms, from the input and output spectra. In the case of a typical modal analysis experiment, a large amount of data is available and some preprocessing of the data is recommended to reduce both the size of the data set and the noise levels before starting the parametric identification of the model parameters.

Therefore, in EMA applications it is common to reduce the amount of data and the noise levels by using the frequency response functions (FRFs) as primary data instead of the input and output spectra. These FRFs are estimated in a non-parametric preprocessing step. The measured forces and vibration responses are divided into different data blocks in order to average and estimate the FRFs. In the case that only limited data is available and averaging reduces the frequency resolution below a critical value, it is advised to start the identification from the raw input spectra and output spectra (I/O based).

From the estimates of the transfer function matrix, i.e. the FRFs, the discussed mathematical model discussed above can be identified.

3.2. Output-only measurements: a stochastic approach

In some applications (e.g. civil engineering [16], in-flight testing [17,18]) one is more interested in obtaining modal models from structures during their operational conditions to model the interaction between the structure and its environment e.g. wind, traffic, boundary conditions, turbulence. Another advantage of an in-operation modal analysis is that nonlinear effects are linearized around the operational working point. For these applications the structures are naturally excited by ambient excitation forces, e.g. wind, traffic, seismic activity (micro-earthquakes), etc. [19,20] which are difficult or even impossible to measure. Elimination of this ambient excitation is often impossible and applying an artificial measurable force which exceeds the natural excitation is expensive and difficult. In these cases, one only measures vibration responses (illustrated by Figure 2).

From this output-only data one can again estimate the natural frequencies, damping values and mode shapes. The knowledge of the input signal is replaced by the assumption that the response is a realization of a stochastic process with unknown white noise as an input. Identifying system parameters from these responses only is referred to as *stochastic system identification* [1,21]. More specific to the identification of vibrating structures the terms *output-only modal analysis* and *in-operation* or *operational modal analysis* (OMA) are commonly used.

3.2.1. Auto/cross-power-density driven stochastic identification

In the field of *stochastic system identification* one can generally divide the identification techniques into two basic subcategories, i.e.

- *Data-driven stochastic identification* algorithms which directly start the identification from the output time sequences or output spectra.
- *Correlation or auto- and cross-spectral-density driven stochastic identification* algorithms which estimate in a first step the covariance or auto- and cross-spectral densities between the outputs and certain reference sensors.

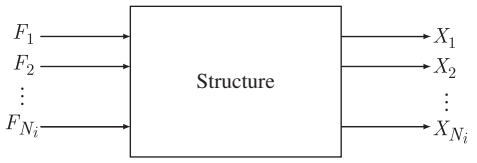

Fig. 1. Deterministic input–output model.

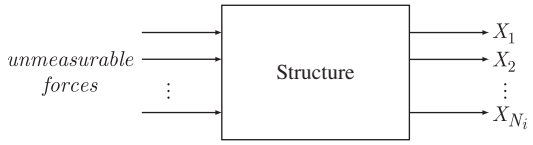

Fig. 2. Stochastic output-only model.

Auto/cross-power-density driven stochastic identification algorithms can be considered as the stochastic counterpart of the FRF-driven deterministic algorithms, since similarly to FRF-driven identification, spectral functions are used as primary data. In fact power-density-based identification methods first estimate power densities between the responses and certain reference responses. In the next step a parametric model is fitted to these functions.

In this paragraph the modal decomposition of power densities and correlations is briefly discussed and references for a more profound discussion are given. It will be shown that under the assumption that the forces are white-noise sequences, the power densities have a modal decomposition that is similar to FRFs.

In Ref. [2] it is shown that for stationary stochastic processes the auto- and cross-spectral densities, also known as power spectra, of the outputs $\mathbf{S}_{yy}(s) \in \mathbb{C}^{N_o \times N_o}$ are given by

$$\mathbf{S}_{yy}(s) = \mathbf{H}(s)\mathbf{S}_{ff}(s)\mathbf{H}(s)^H \tag{11}$$

where $\mathbf{S}_{ff}(s) \in \mathbb{C}^{N_i \times N_i}$ contains the cross-power spectra of the (unknown) input forces. Under the assumption that the forces are white-noise sequences $S_{ff}(s)$ can be considered to be a constant matrix with respect to the frequencies. Consequently, it is shown in Refs. [22,23] that by substituting Eq. (4), in Eq. (11), power densities of the outputs $\mathbf{S}_{yy}(s)$ evaluated at frequency ω can be modally decomposed as follows:

$$\mathbf{S}_{yy}(s) = \sum_{r=1}^{N_m} \left(\frac{\phi_r \mathbf{K}_r^{\mathrm{T}}}{s - \lambda_r} + \frac{\phi_r^* \mathbf{K}_r^H}{s - \lambda_r^*} + \frac{\phi_r \mathbf{K}_r^{\mathrm{T}}}{-s - \lambda_r} + \frac{\phi_r^* \mathbf{K}_r^H}{-s - \lambda_r^*} \right), \tag{12}$$

where $\boldsymbol{\psi}_{[:,r]}$ and $\mathbf{K}_{[:,r]}$ are, respectively, the mode shape and operational reference vector for mode r. This reference vector is a function of the modal parameters and the cross-power spectrum matrix of the unknown random input force(s). Unfortunately, the modal participation factors and by consequence the modal scale factors cannot be determined from a single OMA test.

The problem mentioned above rises when the (unknown) input forces are no longer white-noise sequences, as often is in practice. The latter introduces some additional terms $\boldsymbol{\Theta}_{\mathrm{exc}}$ into the modal decomposition of the power densities that are dependent on the coloring of the unknown input forces [23].

$$\mathbf{S}_{yy}(s) = \sum_{r=1}^{N_m} \left(\frac{\phi_r \mathbf{K}_r^{\mathrm{T}}}{s - \lambda_r} + \frac{\phi_r^* \mathbf{K}_r^H}{s - \lambda_r^*} + \frac{\phi_r \mathbf{K}_r^{\mathrm{T}}}{-s - \lambda_r} + \frac{\phi_r^* \mathbf{K}_r^H}{-s - \lambda_r^*} \right) + [\boldsymbol{\Theta}_{\mathrm{exc}}(s)]. \tag{13}$$

For this reason, additional peaks appear in the power spectra of the responses that are not related to resonance of the system with the already mentioned difficulties. An overview of possible techniques—for the discrimination of true physical modes from peaks related to the excitation—is given in Ref. [24]

3.2.2. Transmissibilities-driven stochastic identification

In this contribution attention will be paid to the use of transmissibilities as primary data to derive modal parameters [25]. Contrary to the classical output-only approach of the previous section, no assumption about the nature of forces will be required. Transmissibilities are obtained by taking the ratio of two response spectra, i.e. $T_{ij}(s) = X_i(s)/X_j(s)$. These transmissibility functions can, in a similar way as FRFs, be estimated in a non-parametric preprocessing step. The measured vibration responses are divided into different data blocks in order to average and estimate the transmissibility functions.

In general, it is not possible to identify modal parameters from transmissibility measurements. By assuming a single force that is located in, say, the input dof k, the transmissibility reduces to

$$T_{ij}(s) = \frac{X_i(s)}{X_j(s)} = \frac{H_{ik}(s)F_k(s)}{H_{jk}(s)F_k(s)} = \frac{B_{ik}(s)}{B_{jk}(s)} \triangleq T_{ij}^k(s), \tag{14}$$

with $B_{ik}(s)$ and $B_{jk}(s)$ the numerator polynomials occurring in the common-denominator models $H_{ik} = B_{ik}(s)/A(s)$ and $H_{jk} = B_{jk}(s)/A(s)$. Note that the common-denominator polynomial, $A(s)$, whose roots are the system's poles, λ_m, disappears by taking the ratio of the two response spectra. Consequently, the poles of the transmissibility function (14) equal the zeroes of transfer function $H_{jk}(s)$, i.e. the roots of the numerator

polynomial $B_{jk}(s)$. So, in general, the peaks in the magnitude of a transmissibility function do not at all coincide with the resonances of the system.

Note that transmissibilities as defined in Eq. (14) depend on the location of the input dof k of the unknown force. The fact that transmissibilities vary with the location of the input forces will implicity be used to find the system's poles.

By making use of the modal model between input dof, k, and, say, output dof, i,

$$H_{ik}(s) = \sum_{m=1}^{N_m} \frac{\phi_{im} L_{km}}{s-\lambda_m} + \frac{\phi_{im}^* L_{km}^*}{s-\lambda_m^*}, \tag{15}$$

one concludes by considering Eq. (14) that the limit value of the transmissibility function (14) for s going to the system's poles, λ_r, converges to

$$\begin{aligned}
\lim_{s\to\lambda_r} T_{ij}^k(s) &= \lim_{s\to\lambda_r} \frac{(s-\lambda_r)H_{ik}(s)}{(s-\lambda_r)H_{jk}(s)} \\
&= \frac{\lim_{s\to\lambda_r} \sum_{m=1}^{N_m} \left(\dfrac{(s-\lambda_r)\phi_{im}L_{km}}{s-\lambda_m} + \dfrac{(s-\lambda_r)\phi_{im}^* L_{km}^*}{s-\lambda_m^*} \right)}{\lim_{s\to\lambda_r} \sum_{m=1}^{N_m} \left(\dfrac{(s-\lambda_r)\phi_{jm}L_{km}}{s-\lambda_m} + \dfrac{(s-\lambda_r)\phi_{jm}^* L_{km}^*}{s-\lambda_m^*} \right)} \\
&= \frac{\lim_{s\to\lambda_r} \dfrac{(s-\lambda_r)\phi_{ir}L_{kr}}{s-\lambda_r} + 0}{\lim_{s\to\lambda_r} \dfrac{(s-\lambda_r)\phi_{jr}L_{kr}}{s-\lambda_r} + 0} \\
&= \frac{\phi_{ir}}{\phi_{jr}}
\end{aligned} \tag{16}$$

and becomes independent of the location of the input dof k of the (unknown) force.

This fact that the transmissibility function becomes independent of the location of the applied force exactly at the system poles can now be used to find the system poles that were canceled out in the previous section.

The subtraction of two transmissibility functions with the same output dofs, (i,j), but with different input dofs, (k,l), of the applied force satisfies

$$\lim_{s\to\lambda_r} (T_{ij}^k(s) - T_{ij}^l(s)) = \frac{\phi_{ir}}{\phi_{jr}} - \frac{\phi_{ir}}{\phi_{jr}} = 0. \tag{17}$$

This means that the system's poles, λ_m, are zeroes of the rational function $\Delta T_{ij}^{kl}(\omega) \triangleq T_{ij}^k(\omega) - T_{ij}^l(\omega)$, and, consequently, poles of its inverse, i.e.

$$\Delta^{-1} T_{ij}^{kl}(s) \triangleq \frac{1}{\Delta T_{ij}^{kl}(s)} = \frac{1}{T_{ij}^k(s) - T_{ij}^l(s)}. \tag{18}$$

The above elaborated theoretical results show that it is possible, by using transmissibilities, to obtain a rational function $\Delta^{-1} T_{ij}^{kl}(s)$, with poles equal to the system's poles. This is directly the result of the fact that transmissibilities vary with the location of the applied forces, but become independent of them at the system's poles and all converge to the same unique value as shown in Eq. (16).

As such, transmissibility driven stochastic identification algorithms can also be considered as a stochastic counterpart of the FRF-driven deterministic algorithms. In both cases, spectral functions are used as primary data. In fact the transmissibility-based identification methods first estimate transmissibility functions between the responses and a certain reference response under one loading condition. By estimating the same set of transmissibility functions under a second loading condition and combining them with the transmissibility functions obtained under the first loading condition one can estimate the $\Delta^{-1} T_{ij}^{kl}(s)$ functions.

In the next step the correct system poles, λ_m, can easily be identified, by identifying the discussed mathematical models from the estimates of the $\Delta^{-1} T_{ij}^{kl}(s)$ functions by performing a parametric estimation, in

a similar way as for the deterministic FRFs (this will be elaborated in more detail in the next section). In this way both the damped resonant frequencies and the damping ratios of each mode in the frequency range of interest can be obtained.

4. Identifying the modal parameters

In previous paragraphs mathematical models to describe the dynamical behavior of the structure and the different types of primary data were discussed. In this section a brief introduction will be given on how identification methods can be used to extract the modal parameters starting from these models and the measured primary data.

Only frequency-domain methods will be considered. These frequency-domain estimators are based on the minimization of an equation error ε between the measured primary data and the mathematical model used [26]. Considering for example the common-denominator description, this equation error is defined as

$$\varepsilon(\omega_f) = H(\omega_f) - \frac{B(\omega_f, \theta)}{A(\omega_f, \theta)}. \tag{19}$$

In this case the primary data consists of FRF measurements where ω_f is the angular frequency ($f = 1, \ldots, N_f$ with N_f the number of measured frequency lines) and the polynomial coefficients θ are the parameters to be estimated.

The quadratic cost function is then defined as the Frobenius norm of the squared error function for each angular frequency ω_f, i.e $l(\theta) = \sum_{f=1}^{N_f} \|\varepsilon(\omega_f)\|_F^2$. The most straightforward method to minimize $l(\theta)$ with respect to the parameters is using a least-squares approach. Based on this idea, a large number of least-squares estimators have been described in the literature during the last two decades [2,3]. All these estimators are in essence curve-fitting techniques.

In this contribution the system poles, λ_m, are identified, by directly applying a frequency-domain estimator [26,27] to the $\Delta^{-1} T_{ij}^{kl}$ functions.

In this case the equation error is defined as

$$\varepsilon(\omega_f) = \Delta^{-1} T(\omega_f) - \frac{B(\omega_f, \theta)}{A(\omega_f, \theta)}. \tag{20}$$

From the identified mathematical model both the damped resonant frequencies and the damping ratios of each mode in the frequency range of interest are obtained.

In the next step it is also possible to obtain unscaled mode shape vectors by curve-fitting the different transmissibility measurements T_{ij} (for $i = 1, \ldots, n$ with n the number of measured output dof) and evaluate them at the previously obtained system poles. This can be verified by looking at Eq. (16), since the values of the transmissibilities at the system poles are directly related to the scalar mode-shape values ϕ_{im} and ϕ_{jm}. By choosing a fixed reference dof j and giving ϕ_{jm} a normalized value of 1, the full unscaled mode-shape vector $(\phi_{1m}, \phi_{2m} \ldots, 1, \ldots, \phi_{nm})$ can be constructed.

Note that the rational function $\Delta^{-1} T_{ij}^{kl}$ can be rewritten as

$$\begin{aligned} \Delta^{-1} T_{ij}^{kl}(s) &= \frac{1}{\dfrac{H_{ik}(s)}{H_{jk}(s)} - \dfrac{H_{il}(s)}{H_{jl}(s)}} \\ &= \frac{H_{jk}(s) H_{jl}(s)}{H_{ik}(s) H_{jl}(s) - H_{il}(s) H_{jk}(s)} \\ &= \frac{B_{jk}(s) B_{jl}(s)}{B_{ik}(s) B_{jl}(s) - B_{il}(s) B_{jk}(s)} \end{aligned} \tag{21}$$

and so, the order of the polynomial, $B_{ik}(s)B_{jl}(s) - B_{il}(s)B_{jk}(s)$, can exceed the order of the common-denominator polynomial, $A(s)$. This means that $\Delta^{-1} T_{ij}^{kl}(s)$ can contain more poles than the system's poles only. Hence, in general, only a subset of the poles of $\Delta^{-1} T_{ij}^{kl}(s)$ will correspond to the real system's poles.

To select the the correct system poles, a singular value decomposition [28] can, for instance, be used. This method will be described in detail in Section 5.

In the next section the new output-only procedure will be illustrated by means of a numerical experiment on a cantilever beam. A comparison will be made between the results of a classic input–output and the new output-only modal analysis based on transmissibility measurements. Eventually, some considerations and conclusions will be given in Sections 6 and 7.

5. Simulation results

Consider the steel cantilever beam given in Fig. 3 with dimensions: $1\,\text{m} \times 0.01\,\text{m} \times 0.01\,\text{m}$.

A Finite Element model is created, using the commercially available software Femlab. In Femlab, a default meshing is applied resulting in 300 elements and the FRFs are calculated, using a direct solver. A total of 4 different experiments are performed, respectively, with a single force applied in the vertical direction in location 0,1,2 and 3, respectively at the free tip and 0.1, 0.3 m and 0.8 m from the free tip. The responses are measured at the same locations 1–3.

Fig. 4 shows the FRFs for a force at location 1. The vertical dashed lines indicate the location of the resonant peaks of the beam (see Fig. 4).

Next, the transmissibility between the responses 2 and 1, T_{21}^{k} is calculated and compared in Fig. 5 for the 4 different locations, $k = 0, \ldots, 3$, of the single force. One notices that the amplitude peaks of the transmissibilities do not correspond with the resonant frequencies. However, all transmissibilities cross each other at the resonant frequencies of the beam, which is in agreement with the theoretical results of Section 3.

Starting from transmissibility measurements under different loading conditions, several $\Delta^{-1}T_{ij}^{kl}$ functions—defined in Eq. (18)—can be computed. These functions are illustrated in Fig. 6 for different combinations of the force locations k and l. It can be observed that most of the amplitude peaks coincide with the resonant peaks of the beam considered.

The correct system poles, λ_m, can now easily be identified, and compared with those obtained from EMA by directly applying a frequency-domain estimator to the transmissibility-based $\Delta^{-1}T_{ij}^{kl}$ functions as well as to the FRFs. The primary data are compared to the identified models in Fig. 7 and demonstrate a perfect fit.

Fig. 3. Cantilever beam.

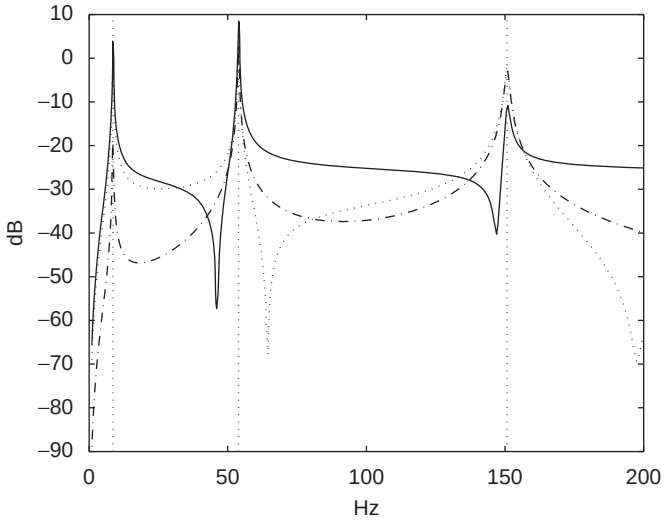

Fig. 4. Frequency response data H_{11}—— H_{21} $\cdots$ H_{31} $-\cdot-$.

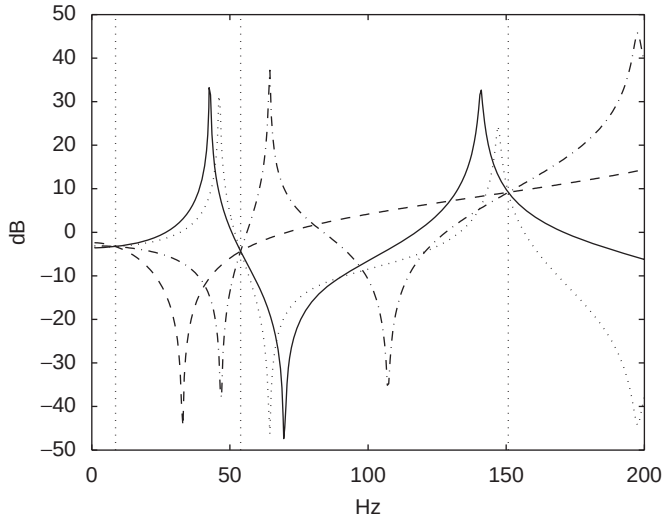

Fig. 5. Transmissibilities T_{21}^{0}——$T_{21}^{1}\cdots T_{21}^{2}$ − · − T_{21}^{3} − −−.

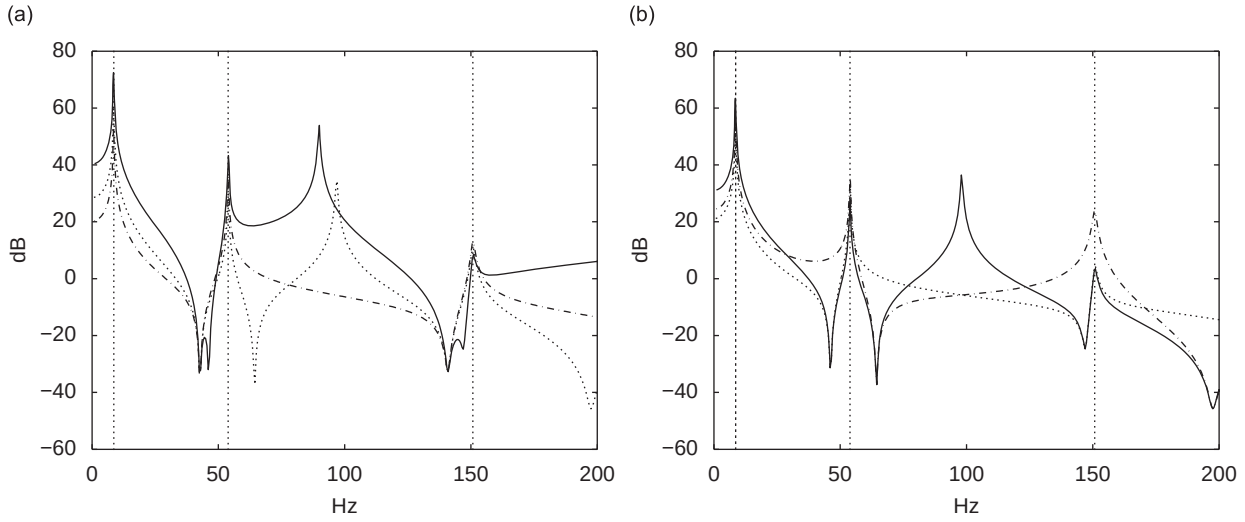

Fig. 6. (a) $\Delta^{-1}T_{21}^{01}$——$\Delta^{-1}T_{21}^{02}\cdots\Delta^{-1}T_{21}^{03}$ − · − (b) $\Delta^{-1}T_{21}^{12}$——$\Delta^{-1}T_{21}^{13}\cdots\Delta^{-1}T_{21}^{23}$ − · −.

The identified damping ratios and damped natural frequencies are summarized in Table 1.Both approaches—frequency response and transmissibility-based—yield identical results. The transmissibility-based approach results in additional poles that are not related to the system's dynamics. This is a direct result of the fact that the order of the $\Delta^{-1}T_{ij}^{kl}$ can exceed the order of the common-denominator polynomial, $A(s)$, as was explained in Section 4. One can also understand this by looking at Fig. 5, where one can see that the transmissibility functions obtained from 2 different loading conditions k can have more crossings then there are poles in the frequency band of interest. As such the calculated $\Delta^{-1}T_{ij}^{kl}$ can have more peaks than there are system poles. This can be observed in Fig. 6.

In what follows, a mathematical tool that helps to distinguish the real system poles from the additional ones will be elaborated. The idea is to consider also a third loading condition and to evaluate more than 2 transmissibility functions at the same time, which is currently the case if only the calculated $\Delta^{-1}T_{ij}^{kl}$ functions

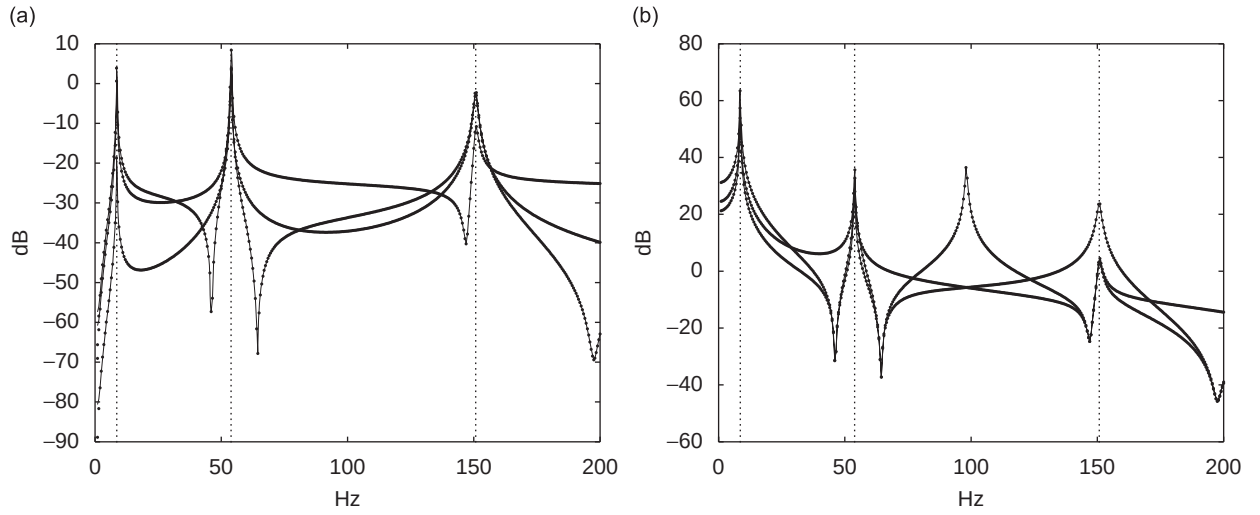

Fig. 7. Comparison between the estimated model (full line) and the measured spectra (dots) of (a) the FRFs and (b) the $\Delta^{-1}T_{ij}^{kl}$ functions.

Table 1
Comparison of the estimated damping ratios and damped natural frequencies obtained from the FRF measurements and the transmissibility-based approach

$\zeta(H)(\%)$	$\zeta(\Delta^{-1}T)(\%)$	$f_d(H)$ (Hz)	$f_d(\Delta^{-1}T)$ (Hz)
0.027	0.027	8.602	8.602
0.169	0.169	53.88	53.88
—	0.308	–	98.11
0.474	0.474	150.8	150.8

are considered. The easiest way to achieve this goal is by considering the following square matrix and to evaluate its rank.

$$[T(s)] = \begin{bmatrix} T_{21}^1(s) & T_{21}^2(s) & T_{21}^3(s) \\ 1 & 1 & 1 \\ 1 & 1 & 1 \end{bmatrix}. \tag{22}$$

The proposed matrix is of rank 2, since it has two equal rows of ones. If only 2 out of the 3 transmissibility functions are equal the matrix remains of rank 2. If all 3 transmissibility functions are equal the matrix will become of rank 1. An easy way to evaluate the rank of a matrix is by performing a singular value decomposition [28]. If a 3×3 matrix is of rank 3 it has 3 singular values that differ from 0. If the matrix is of rank 1, only the first singular value will be different from 0.

Considering the fact that all transmissibility functions converge to the same unique values at the system poles (16), all columns of this matrix will become equal at the system poles. Thus the proposed matrix will be of rank 1 at the system poles, λ_m. This implies that the second singular value $\sigma_2(s)$ should converge to 0 for $s = \lambda_m$.

If the experiment performed allows to measure more transmissibility functions one can extend the previous matrix to, e.g., Eq. (23), which further reduce the risk of finding additional poles. In this case the condition necessary for the matrix to become of rank 1 is that 2 times 3 transmissibility functions converge to the same value.

$$[T(s)] = \begin{bmatrix} T_{21}^1(s) & T_{21}^2(s) & T_{21}^3(s) \\ T_{31}^1(s) & T_{31}^2(s) & T_{31}^3(s) \\ 1 & 1 & 1 \end{bmatrix}. \tag{23}$$

This matrix should also be of rank 1 at the system poles, λ_m, implying that the singular value $\sigma_2(s)$ should converge to 0 for $s = \lambda_m$.

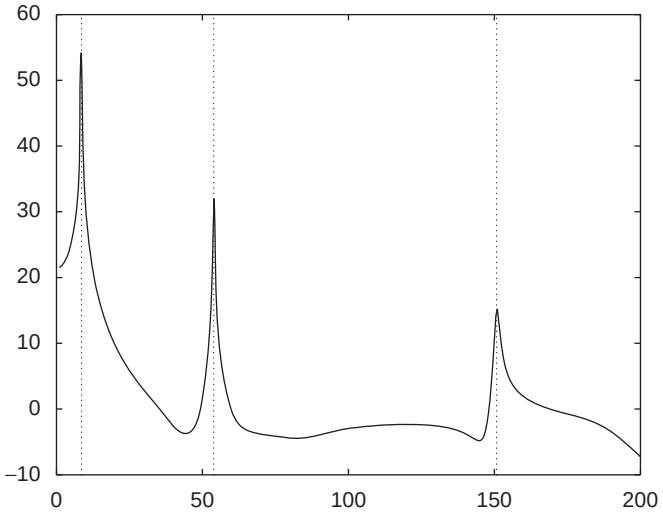

Fig. 8. Selection of the system's poles by means of a sigular value decomposition $1/\sigma_2(\omega)$—.

One can also calculate the matrix (23) in the frequency domain by replacing s with ω_f ($f = 1, \ldots, N_f$ with N_f the number of measured frequency lines). For a weakly damped system, $\lambda_m \approx \mathrm{j}\omega_m$, (as often is the case in mechanical structures) this matrix should be of rank 1 at the resonant frequencies ω_{dm}, implying that the second singular value $\sigma_2(\omega_f)$ should converge to 0 for $\omega_f = \omega_{dm}$. In Fig. 8, $\sigma_2(\omega_f)$ is plotted as a function of frequency. One can see that only 3 peaks coinciding with the resonant frequencies are present.

Once the resonant frequencies are known, it is possible to derive the (operational) mode shapes from the transmissibilities as was explained in Section 4. Fig. 9 shows the comparison between the modes obtained from the FRFs as primary data and those obtained using the transmissibility measurements.

6. Some considerations

The example above was elaborated assuming a single input excitation. However, in real operational conditions we mostly deal with a multiple-input situation. In general an unknown number of simultaneous sources are exciting the structure, some of which may be distributed.

In this situation the transmissibility reduces to

$$T_{ij}(s) = \frac{X_i(s)}{X_j(s)} = \frac{\sum_{k=1}^{n} H_{ik}(s)F_k(s)}{\sum_{k=1}^{n} H_{jk}(s)F_k(s)} = \frac{\sum_{k=1}^{n} B_{ik}(s)F_k(s)}{\sum_{k=1}^{n} B_{jk}(s)F_k(s)}, \tag{24}$$

with n the number of forces applied to the structure. Also in this case the common-denominator polynomial, whose roots are the system poles, disappears. In order to show that the transmissibility OMA procedure elaborated above can still be used in the presence of multiple inputs, it is sufficient to demonstrate that the transmissibility functions as defined in Eq. (24) with the same output dofs, (i,j), but with different forces $F_k(\omega)$ still converge to the same unique value at the system poles.

Note that it is no longer possible to eliminate the forces $F_k(\omega)$, and so the transmissibility function (24) not only depends this time on the location but also on the amplitude of those forces. Nevertheless, in Eq. (25) one can still verify that the transmissibility functions for different forces (e.g. different locations of the forces, different number of forces or different amplitudes of the forces) still converge to the same unique value at the system poles, and therefore the proposed technique is still applicable.

$$\lim_{s\to\lambda_r} T_{ij}(s) = \frac{\sum_{k=1}^{n} \lim_{s\to\lambda_r}(H_{ik}(s)F_k(s))}{\sum_{k=1}^{n} \lim_{s\to\lambda_r}(H_{jk}(s)F_k(s))} = \frac{\sum_{k=1}^{n} \phi_{ir}L_{kr}F_k(s)}{\sum_{k=1}^{n} \phi_{jr}L_{kr}F_k(s)}$$

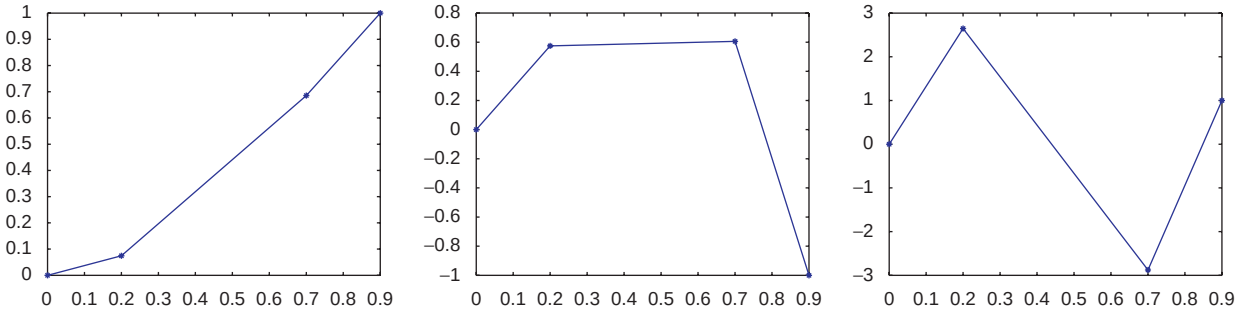

Fig. 9. Comparison between unscaled mode shapes from FRFs (dots) and transmissibility measurements (full line).

$$= \frac{\phi_{ir} \sum_{k=1}^{n} L_{kr} F_k(s)}{\phi_{jr} \sum_{k=1}^{n} L_{kr} F_k(s)}$$

$$= \frac{\phi_{ir}}{\phi_{jr}}, \tag{25}$$

This shows the robustness of the method since it demonstrates that the procedure is not harmed by the fact that we have several forces exciting the structure simultaneously. These forces do not need to be known and are allowed to be distributed.

In order to use the transmissibility OMA procedure in operational conditions with a multiple inputs or distributed loads, it is sufficient that the loads change in position, amplitude or number of applied loads. These different loading conditions can be obtained by, e.g. a change in the ambient forces (e.g. change of wind-level/wind-direction) or by adding artificial applied forces (e.g. impact hammer) in different locations. One can also consider a loading condition resulting from both artificial applied forces and unknown ambient excitation.

7. Conclusions

A comparison was made between identification results of a classic input–output modal analysis using FRFs as primary data and the new proposed output-only technique using transmissibility measurements as primary data. It has been shown in this paper that the correct system poles can be identified starting from transmissibility measurements only. Classical output-only techniques often require the operational forces to be white noise. This is not necessary for the proposed transmissibility-based approach. The unknown operational forces can be arbitrary (colored noise, swept sine, impact, etc.) as long as they are persistently exciting the structure in the frequency band of interest. In order to use the proposed method it is necessary that different loading conditions can be obtained during the experiment.

Acknowledgments

This research has been supported by the Institute for the Promotion of Innovation by Science and Technology in Flanders (IWT), the Fund for Scientific Research-Flanders (Belgium) (FWO) and by the Research Council (OZR) of the Vrije Universiteit Brussel (VUB).

References

[1] P. Van Overschee, B. De Moor, *Subspace Identification for Linear Systems: Theory-Implementation-Applications*, Kluwer Academic Publischers, Dordrecht, 1996.
[2] L. Ljung, *System Identification: Theory for the User*, Prentice-Hall, Englewood Cliffs, NJ, 1999.
[3] R. Pintelon, J. Schoukens, *System Identification: A Frequency Domain Approach*, IEEE Press, John Wiley, New York, 2001, ISBN 0-7803-6000-1.
[4] W. Heylen, S. Lammens, P. Sas, *Modal Analysis Theory and Testing*, K.U.Leuven, Belgium, 1997.

[5] N.M.M. Maia, J.M.M. Silva, (ed.), *Theoretical and Experimental Modal Analsysis*, Research Studies Press Ltd., Somerser, England, 1997, ISBN 0-86380-208-7.
[6] D. Ewins, *Modal Testing: Theory and Practice*, Research Studies Press, Letchworth, Hertfordshire, UK, 1986.
[7] B. Cauberghe, Applied Frequency-domain System Identification in the Field of Experimental and Operational Modal Analysis. PhD Thesis, Department of Mechanical Engineering, Vrije Universiteit Brussel, Belgium, 2004, phd.avrg.be.
[8] P. Guillaume,L. Hermans, H. Van der Auweraer, Maximum Likilihood identification of modal parameters from operational data, *Proceedings of the 17th International Modal Analysis Conference (IMAC17)*, 1999, pp. 1887–1893.
[9] E. Parloo, P. Guillaume, B. Cauberghe, Maximum Likelihood identification of non-stationary operational data, *Journal of Sound and Vibration (JSV)* 262 (1) (2003) 161–173.
[10] L. Hermans, H. Van der Auweraer, Modal testing and analysis under operational conditions: industrail applications, *Mechanical Systems and Signal Processing* 13 (2) (1999) 193–216.
[11] P. Mohanty, D.J. Rixen, Operational modal analysis in the presence of harmonic excitations, *Journal of Sound and Vibration* 270 (1–2) (2004) 93–109.
[12] N.J. Jacobsen, Identifying harmonic components in operational modal analysis. *Twelfth International Congress on Sound and Vibration*, Lisbon, Portugal, July 2005.
[13] N.J. Jacobsen, P. Andersen, R. Brinker, Using enhanced frequency domain decomposition as a robust technique to harmonic excitation in operational modal analysis, *International Conference on Noise and Vibration Engineering (ISMA)*, Leuven, Belgium, September 2006.
[14] P. Mohanty, D.J. Rixen, Modified era method for operational modal analysis in the presence of harmonic excitations, *Mechanical Systems and Signal Processing* 20 (1999) 114–130.
[15] P. Mohanty, D.J. Rixen, A modified Ibrahim time domain algorithm for operational modal analysis including harmonic excitation, *Journal of Sound and Vibration* 275 (1–2) (2004) 375–390.
[16] B. Peeters, G. De Roeck, Stochastic system identification for operational modal analysis: a review, *Measurement and Control* (2001) 623–659.
[17] M. J Brenner, R.C. Lind, D.F. Vorafeck, Overwiew of recent flight flutter testing, *Journal of Aerospace Engineering* (1995) 209.
[18] M.W. Kehoe, A historical Overview of light flutter testing, *NASA Technical Memorandum* 25 (1995) 4720.
[19] M.F. Green, Modal test method for bridges: a review. *Proceedings of the 14th International Modal Analysis Conference (IMAC14)*, 1995, pp. 552–558.
[20] C.R. Farrar, T.A. Duffey, P.J. Cornwell, S.W. Doebling, Excitaton methods for bridge structures. *Proceedings of the 17th International Modal Analysis Conference (IMAC17)*, Kissemmee (FL), USA, 1999, pp. 1063-1068.
[21] B. Peeters, System Identification and Damage Detection in Civil Engineering. PhD Thesis, Department of Civil Engineering, Katholieke Universiteit Leuven, Belgium, 2000.
[22] L. Hermans, H. Van der Auweraer, P. Guillaume, A frequency-domain maximum likelihood approach for the extraction of modal parameters from output-only data. *Proceedings of the 23th International Seminar on Modal Analysis, Leuven, Belgium*, September 1998.
[23] E. Parloo, Application of Frequency-domain System Identification Techniques in the Field of Operational Modal Analysis. PhD Thesis, Department of Mechanical Engineering, Vrije Universiteit Brussel, Belgium, 2003, avrg.vub.ac.be.
[24] W. Lisowski, Classification of vibration modes in operational modal analysis, *Proceedings of the International Conference on Structural System Identification, Kassel, Germany* 2001, pp. 593-602.
[25] P. Guilaume, C. Devriendt, G. De Sitter, Identification of modal parameters from transmissibility measurements; *First International Operational Modal Analysis Conference*, Copenhagen, Denmark, April 2005.
[26] R. Pintelon, P. Guillaume, Y. Rolain, J. Schoukens, H. Van Hamme, Parametric identification of transfer functions in the frequency domain: a survey, *IEEE Transactions on Automatic Control* 39 (11) (1994) 2245–2260.
[27] B. Peeters, H. Van der Auweraer, P. Guilaume, J. Leuridan, The PolyMAX frequency-domain method: a new standard for modal parameter estimation?, *Shock and Vibration* 11 (2004) 395–409.
[28] G. H Golub, C.F. VanLoan, *Matrix Computations*. third ed., Johns Hopkins University Press, Baltimore. 1999, ISBN 0-8018-5414-8.